MECHANISM OF METHANE-AIR COMBUSTION ON THE SURFACE OF A POROUS CERAMIC PLATE

YASUHISA NAKAMURA, YOSHINORI ITAYA,
KAZUHITO MIYOSHI AND MASANOBU HASATANI*
Department of Chemical Engineering, Nagoya University, Nagoya 464

Key Words: Combustion, Energy, Heat Transfer, High Temperature, Methane-Air Flow, Porous Plate, Radiation, Ceramic Burner

The mechanism of mathane-air combustion on the surface of a porous ceramic plate was studied by experimental testing and analysis of a simplified theoretical model based on one-dimensional flow of methane-air mixture and the overall chemical reaction rate.

The effects of such parameters as thickness of porous ceramic plates, equivalence ratio of mixed-gas and heat load on the combustion characteristics were examined.

A thicker plate achieves higher surface temperature as premixed gas is preheated on the porous ceramic plate. The combustion zone is closest to the porous ceramic plate with equivalence ratio $\Phi = 1.2$. The surface temperature has peak value at a certain heat load. It is observed that combustion begins just off the porous ceramic plate, and the flame is kept less than 1mm from the surface. The position is influenced by the combustion conditions. These phenomena can be explained by a theoretical model and such aspects of the combustion mechanism as temperature profile of premixed gas and porous plate and chemical reaction on the plate are made clear.

Introduction

Growing attention to problems affecting the global environment has been promoting extensive studies related to the development of integrated combustion technologies to achieve still higher levels of efficiency and reduction of pollutants. Surface combustion burners of premixed fuels attract much attention as an integrated combustion system that is expected to have attractive characteristics for various applications[12, 14].

Surface combustion burners are designed to form a thin flame zone close to the surface of porous ceramics. This makes possible a compact heating system and highest heat transfer effect due to increasing radiative energy from the porous ceramic plates. The features of combustion behavior of a methane-air flame on the surface of a porous ceramic plate has been examined by the present authors[3]. A thin open flame was formed stably not further than one millimeter from the surface in a wide range of equivalent ratio and heat load, and the solid surface achieved a temperature higher than 900K. However, the surface temperature was influenced by the flame position, which in turn was dependent on the surface temperature and the gas flow rate. This is because the plate surface is heated by the combustion heat and unburnt gas is preheated by the porous ceramics and/or self-generated heat downstream, and is finally ignited in the flame zone close to the surface. Those flame structures are not explained by the conventional theory[1, 10, 11] of the premixed laminar flame unless effects of the solid surface on heat transfer and chemical reaction are involved. In this regard, some recent researches take account of the effect of porous plate on the combustion but those are supposed to form flame at the fixed position in the porous media[2, 15].

In this paper, the combustion mechanism of methane-air flame is studied with no assumption of flame position The theoretical model of the premixed laminar flame was modified to take account of the effect of the surface wall on heat transfer and reaction rate in the stream of premixed gas until ignition. The stability and structure of the flame formed on the ceramic surface are discussed, comparing the analytical result and the experimental result.

* Received October 1, 1992. Correspondence concerning this article should be addressed to M. Hasatani.

1. Theoretical Analysis

1.1 Theoretical model

A theoretical analysis was developed to examine the combustion mechanism of a premixed methane-air flame on a porous ceramic plate placed horizontally in an open atmosphere.

A theoretical model was constructed on the basis of the following assumptions.

(1) One-dimensional piston flow

(2) One-dimensional steady premixed combustion

(3) Overall combustion reactions based on

$$CH_4 + 2O_2 \rightarrow CO_2 + 2H_2O \quad (1)$$

(4) Dispersion of chemical species in the gas flow being ignored

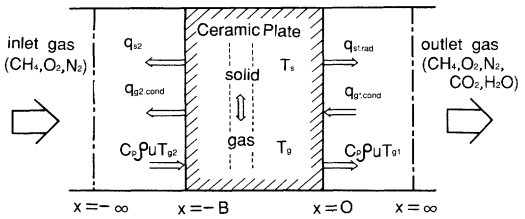

Fig. 1 Model of theoretical analysis

(5) Porous ceramic plate having gray surface for radiative heat transfer
(6) Porous ceramic plate consisting of spherical particles that are uniform in diameter and dispersed uniformly
(7) Both combustion gas and premixed-gas being non-radiant gases
(8) The gases being ideal gases
(9) Radiative heat transfer in porous ceramics being taken account as terms of the effective heat conductivity

The features of the analytical model and the coordinate system for the surface combustion burner are drawn conceptually in **Fig. 1**. Based on those assumptions and the analytical model in Fig. 1, the model of the premixed laminar flame was modified.

1.2 Basic equations

A set of basic equations was derived as follows. The equation for continuity is given by

$$\rho_g u = G_o \tag{2}$$

The equation for heat transfer on the upstream side of the porous ceramic plate (x < –B) is given by

$$C_{Pg}\rho_g u\frac{\partial T_g}{\partial x} - \lambda_g\frac{\partial^2 T_g}{\partial x^2} = R\Delta H \tag{3}$$

where the first term on the left-hand side represents heat capacity of the gas, the second term heat conduction; the term on the right-hand side represents heat generated by reactions. The boundary conditions were

$$X = -\infty;\ T = T_o \tag{4}$$

In the section in which the porous ceramic plate is placed (–B < X < 0), the heat balance equations for the solid and gas sides are given respectively by

$$\lambda_e\frac{\partial^2 T_s}{\partial x^2} = -h_P(T_g - T_s)S \tag{5}$$

and

$$C_{Pg}\rho_g u\frac{\partial T^g}{\partial x} = -h_P(T_g - T_s)S + \varepsilon_p R\Delta H \tag{6}$$

where the right-hand side in Eq. (5) is the convection term between the solid and the gas, and λ_e at the left-hand side represents the effective thermal conductivity of the solid which includes radiative heat transfer in the porous ceramic plate.

Supposing that heat transferred by conduction in the gas stream might be caught by the solid on both plate surfaces, the boundary conditions are derived as:

$$x = -B:\ -\lambda_e\frac{\partial T_s}{\partial x} + \varepsilon\sigma(T_{S2}^4 - T_o^4) + \lambda_g\frac{\partial T_g}{\partial x} = 0 \tag{7}$$

$$x = 0:\ -\lambda_e\frac{\partial T_s}{\partial x} + \varepsilon\sigma(T_a^4 - T_{S1}^4) + \lambda_g\frac{\partial T_g}{\partial x} = 0 \tag{8}$$

where Ta represents the atmospheric temperature.

The heat balance equation downstream of the porous ceramic plate (0 < X) is given by

$$C_{Pg}\rho_g u\frac{\partial T_g}{\partial x} - \lambda_g\frac{\partial^2 T_g}{\partial x^2} = R\Delta H \tag{9}$$

The conservation equations of chemical species for the three sections are given by

$$\rho_g u\frac{\partial Y_j}{\partial x} + R_j M_j = 0 \qquad (x < -B) \tag{10}$$

$$\rho_g u\frac{\partial Y_j}{\partial x} + \varepsilon_P R_j M_j = 0 \qquad (-B < x < 0) \tag{11}$$

$$\rho_g u\frac{\partial Y_j}{\partial x} + R_j M_j = 0 \qquad (x > 0) \tag{12}$$

Their boundary conditions are

$$x = -\infty:\ Y_j = Y_{j,o} \tag{13}$$

The chemical reaction rate of combustion could be estimated as

$$R = [CH_4]\,[O_2]\,T_g^{\alpha}A_o exp\left[\frac{-E_o}{R_g T_g}\right] \tag{14}$$

For the reaction rate constants the following values are used, based on the literature[8]:

$$\begin{aligned}\alpha &= 0\\ A_o &= 0.197\times 10^{16}\quad cm^3/mole\cdot\sec\\ E_o &= 167472\,J/mole\end{aligned} \tag{15}$$

Reaction rates of combustion are generally reduced in small pores of a porous ceramic plate since the radical species are dissipated on the solid wall. To describe the influence in the present analysis, the frequency factor A_0 in Eq. (14) was modified rather than the activation energy E_0. This modification is reasonable because the reaction rates are influenced by the low frequency of collisions in the porous ceramic plate among chemical species with energy higher than the activation energy, which is supposed to be unchanged even in the porous plate. The value is decreased to obtain a stable numerical solution with no divergence, which is reasonable from the theoretical viewpoint because of the low frequency of collision.

$A_0' = 0.197*10^{15}\mathrm{cm^3/mole\cdot sec}$

1.3 Numerical calculation

Numerical solutions were obtained by an iteration method after transforming the basic equations into dimensionless expressions*. To reduce the CPU time the iteration was carried out with constant properties independent of temperature in the first step of the calculation. Then, using the steady solution obtained as the initial distributions, the iteration taking account of the temperature dependency of properties was repeated until

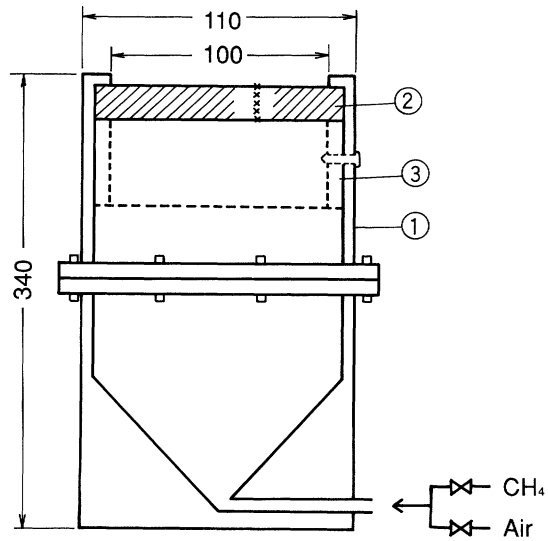

Fig. 2 Experimental apparatus

it converged within a relative accuracy of 10^{-5}.

2. Experimental Apparatus and Procedures

2.1 Experimental apparatus

The combustion system used in the present study is shown in **Fig. 2**. The burner consisted mainly of a porous ceramic plate fixed with stoppers to a stainless steel tube 110 mm in O.D. and 104 mm in I.D. The effective diameter of the combustion area on the surface of the porous ceramic plate was 100 mm and the premixed methane-air gas was fed from the bottom of the burner. To eliminate leakage of the gas, the gap between the burner tube and the porous ceramic plate was sealed with castable when installing the plate. For the material of the porous ceramic plates, silica-alumina was chosen and its properties are as follows:

Porosity: 0.32

Mean pore diameter: 400μm

Emissivity: 0.75[7] (for the oxidized face of aluminum and silicon)

Thermal conductivity: 0.37 $Wm^{-1}K^{-1}$.

The porous ceramic plates were molded to 103±1 mm in diameter and 5 mm/20 mm thick.

2.2 Experimental method

The premixed methane-air gas fed from the bottom was ignited on the surface of the porous ceramic plate, followed by modulation of the gas flow to attain stable combustion at a given condition. The temperature distributions and chemical composition distributions were measured[2]. To measure the temperature on the surface and inside the porous ceramic plate, holes of 1 mm diameter to specified depths were made and 50μm PR thermocouples were inserted in them. Gas temperature was measured at points toward the downstream side of the surface by traversing a 50μm thermocouple set horizontally. The PR thermocouples used in the experiment were coated with silica to prevent catalytic reaction on them.

For chemical composition distributions on the downstream side of the surface of the porous ceramic plate, combustion gas was sampled, using a quartz glass sampling probe 2.7 mm in I.D. The H_2O concentration was determined by letting the vapor in the sampled gas be absorbed into magnesium perchlorite of 10–24 mesh and measuring the change in net weight. Other component concentrations were measured by a gas chromatograph (Yanagimoto G3800).

Table 1.

	a	$b\times10^2$	$c\times10^5$	$d\times10^9$
N_2	28.772	−0.15643	0.8044	−2.8597
O_2	25.362	1.5134	−0.7123	1.3058
CO_2	22.157	5.9540	−3.4853	7.4357
H_2O	32.094	0.19148	1.0508	−3.4957
CH_4	19.798	5.0016	1.2629	−10.9618

3. Results

3.1 Physical properties used for analysis

The temperature dependency of physical properties used in the present theoretical analysis was estimated as follows.

The relationship between heat capacity of gas and temperature could be empirically expressed by[4]

$$C_{pgi} = a_i + b_i T + c_i T^2 + d_i T^3$$

where C_{pgi} denotes heat capacity of i gas component by kJ/kg-mol.K. a_i, b_i, c_i, and d_i are constants and are listed in **Table 1**. The heat capacity of gas mixture is calculated from the fraction of each component by

$$C_{pg} = \sum_i C_{Pgi} M / Y_i \qquad (16)$$

Reaction heat is also a function of temperature. Temperature dependency of enthalpy difference between reactants (A) and products (B) is expressed at a constant pressure as[5]

$$\left(\frac{\partial \Delta H}{\partial T}\right)_p = C_{pB} - C_{pA} = \Delta C_p \qquad (17)$$

Thus, reaction heat is given against temperature as

$$\Delta H = \Delta H_o + \int_{T_o}^{T} \Delta C_p dT \qquad (18)$$

where ΔH_o is reaction heat at the standard state. The effective heat conductivity of the porous ceramics is predicted by Yagi, Kunii and Wakao's relation[13]. The heat conductivity of gas mixture is correlated by Wassiljewa's equation[9] and the convective heat transfer coefficient between solid and gas is decided on the basis of that in the porous media[6].

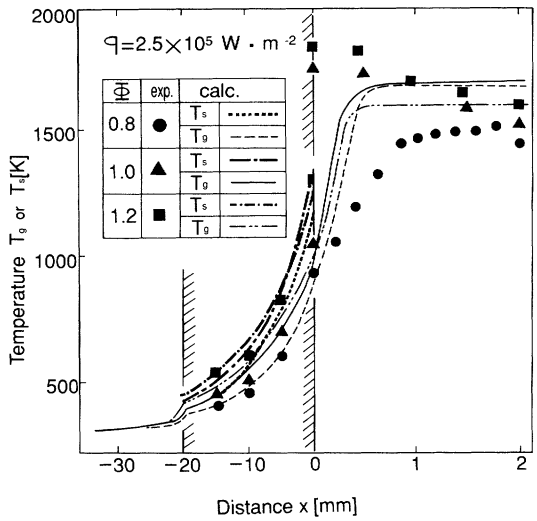

Fig. 3 Temperature distribution in vertical direction along gas stream (Effect of equivalence ratio)

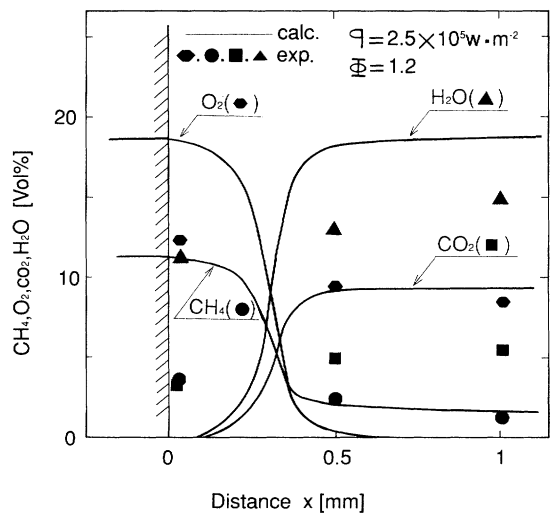

Fig. 4 Distribution of combustion gas component along gas stream ($\Phi = 1.2$)

3.2 Effect of parameters

(a) Equivalence ratio **Figure. 3** shows both the theoretical and experimental temperature distributions of the gas along the gas stream line. The distribution of the solid side is also included inside the porous ceramic plate of $-20 < x < 0$. Both results show that the premixed methane-air gas is preheated in the porous ceramic plate and then rapidly heated up just outside the plate, resulting in the onset of combustion reactions. The temperature of the surface of the porous ceramic plate is theoretically the highest at $\Phi = 1.0$, which is a stoichiometric composition. In the experimental results, however, the temperature is highest at $\Phi = 1.2$. This may be due to the effect of atmospheric air surrounding the burner;, i.e. twenty percent of input methane is unburnt for $\Phi = 1.2$ in the present analytical model, while a combined premixed and diffusion flame is actually formed on the ceramic surface as discussed in the previous paper[3] and would allow the surface temperature to reach maximum as the result of more complicated phenomena

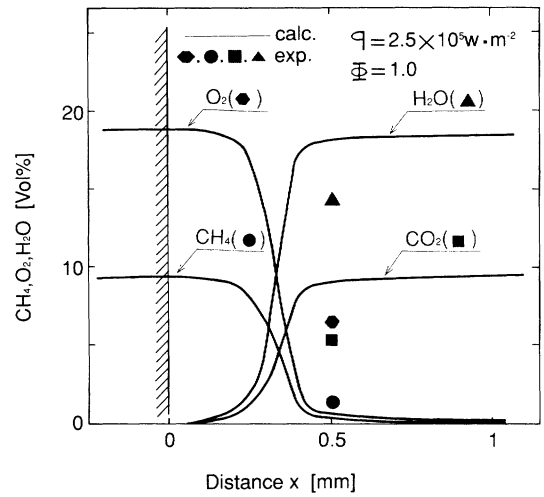

Fig. 5 Distribution of combustion gas component along gas stream ($\Phi = 1.0$)

than those taken into account in the model. Inside the porous ceramic plate, the experimental solid temperatures are smaller than the theoretical values. This is because it is difficult to measure the true solid temperature separated from gas temperature in the porous material where a gas is passing through. Comparing theoretical results with experimental results for combustion gas temperature just off the plate, the experimental results are higher at $\Phi = 1.2$ and lower at $\Phi = 0.8$ than the theoretical results. This may be because, with $\Phi = 1.2$ in this experiment, the excess methane in the premixed gas also burns near the surface of the porous ceramic plate as is shown in **Fig. 4**, where there is combustion with secondary air owing to the decrease in CH_4 and O_2 and the increase in CO_2, H_2O. With $\Phi = 0.8$, the flame lifts slightly and the mixture between combustion gas and atmospheric air becomes significant, yielding experimental results lower than the theoretical values obtained with the assumption of being adiabatic in the downstream gas phase.

The results of theoretical calculations show that the combustion zone is closest to the surface of the porous ceramic plate at $\Phi = 1.2$, although the difference between $\Phi = 1.0$ and $\Phi = 1.2$ is not clear in Fig. 3. But as the point of rapid increase of CO_2, H_2O in Fig. 4 is a little closer to the surface than that in Fig. 5, the flame zone for $\Phi = 1.2$ is supposed to be a little closer than that for $\Phi = 1.0$ This trend corresponds with the agreement with experimental results whose details were also described in the previous paper.

Figures 4 through **6** show the composition distributions for $\Phi = 1.2$, 1.0, and 0.8 respectively of combustion gas downstream of the surface of the porous ceramic plate. Theoretical data show that the combustion zone where O_2 and CH_4 concentrations decrease rapidly is slightly away from the surface of the porous ceramic plate. It is clearly indicated in these figures that the position is getting closer to the surface with increase in the equivalence ratio up to 1.2.

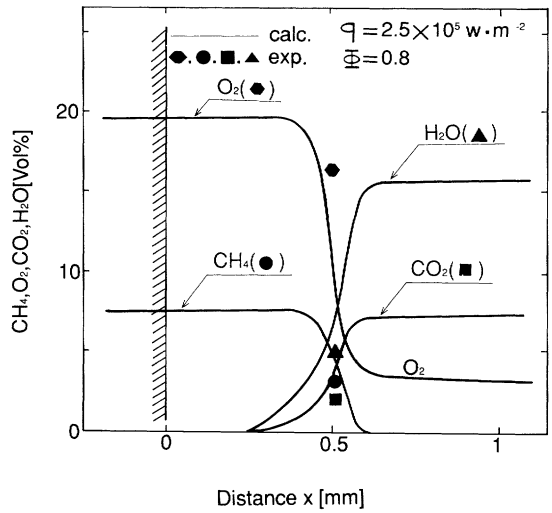

Fig. 6 Distribution of combustion gas component along gas stream ($\Phi = 0.8$)

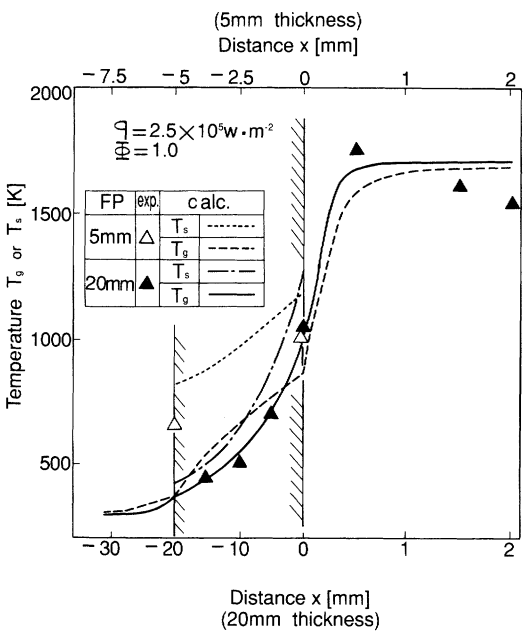

Fig. 7 Temperature distribution in vertical direction along gas stream

Although experimental data in Figs. 4 through 6 are not so accurate owing to difficulty in measurement, the trend that the O_2 concentration for $\Phi = 1.0$ is less than that for $\Phi = 0.8$, is easily explained and the higher O_2 concentration for $\Phi = 1.2$ than expected shows atmospheric air in this case.

(b) Thickness of porous ceramic plate **Figure 7** shows the effect of plate thickness on temperature distributions in the direction of the combustion gas flow. The thicker the porous ceramic plate, the higher the surface temperature. This is because the plate surface is cooled by the premixed gas supplied from the bottom. The combustion zone, where the temperature of the gas coming out of the porous ceramic plate rises sharply, is closer to the surface with a thicker plate. Those experimental trends are simulated successfully by the present theoretical calculation.

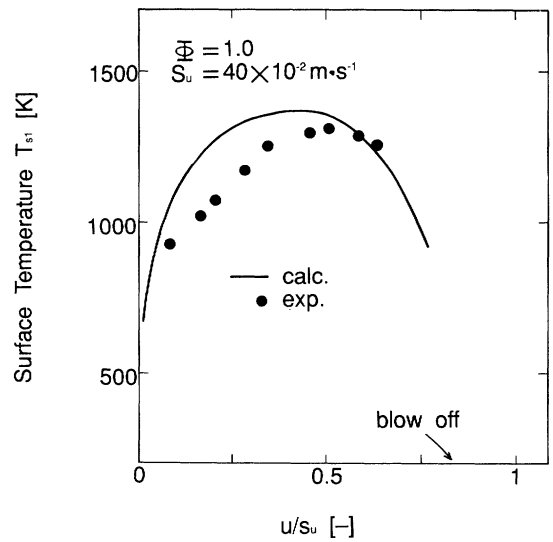

Fig. 8 Surface temperature of porous ceramic plate

(c) Combustion load **Figure 8** shows the relation between superficial gas velocity normalized by the premixed laminar flow propagation velocity[10] of methane-air flame and surface temperature of the porous ceramic plate for $\Phi = 1.0$. Both experimental and theoretical results show that the surface temperature achieves a peak at $u/S_u = 0.5$. This phenomenon could be realized as follows. Radiant heat loss from the surface increases remarkably with a rise in surface temperature, and the flame temperature is reduced from adiabatic flame temperature. At the right-hand side of the peak, the gas flow velocity gradually approaches the flame propagation velocity with increase in u/S_u. This causes the flame position to lift from the surface because the actual combustion velocity on the surface could be less than Su because of the heat loss. Thus the surface temperature begins to decrease although the heat load rises.

4. Discussion

In the previous paper[3], some of the present authors experimentally reported the significant influence of parameters on the combustion characteristics of methane-air on a porous ceramic plate, and pointed out that the premixed flame is stably formed not on or inside the porous plate but at a position less than one millimeter from the surface depending upon conditions Studies have also been made on the combustion mechanism from the concept of heat balance and reaction rate. It was found that an ignited flame downstream of a porous plate propagates upstream if the flame velocity is faster than the gas flow velocity. When the flame approaches the plate surface, the surface temperature rises and heat is released there by radiant heat loss. This allows the combustion velocity as well as the flame temperature to decrease. As a result, the flame is finally kept at an appropriate position where combustion velocity is balanced with gas flow rate above the plate surface. That is

the reason why flashbacks to the rear of the porous plate are rarely observed for this type of burner.

In the present paper, a simple model was developed to ensure that a flame could be stably formed on a porous plate surface by the above-mentioned mechanism. It is noticed that a steady solution, by which the trends of combustion characteristics could be explained, although agreement with experimental data is not yet satisfactory, was obtained from the basic equation developed on the strength of relatively simple assumptions as those described in the theory. The results of theoretical calculations in Figs. 3 through 7 also show that the flame is lifted less than 1 mm from the surface, corresponding to the experimental results.

Conclusions

(1) As the porous ceramic plate contributes to preheating of premixed gas, the surface temperature increases with increase in ceramic plate thickness.
(2) It was observed by results of both surface temperature and exhaust gas composition that the combustion zone is closest to the porous ceramic plate at $\Phi = 1.2$ among the three equivalence ratios.
(3) The higher heat load allows flame to be kept closer to the surface and a higher surface temperature. Once it exceeds the peak point, as the gas velocity increases faster than the combustion velocity at the surface the combustion zone recedes from the surface of the porous ceramic plate, resulting in a drop in surface temperature.
(4) The experimental trends were simulated with relatively good agreement by the theoretical calculation.
(5) Flame is kept at a balancing point of the combustion velocity and gas flow velocity in the downstream flow less than 1 mm from the surface.

Appendix

Dimensionless form

The governing equations in section 2.2 can be rewritten to the following dimensionless expressions. Heat transfer equations are expressed as gas phase:

$$-\infty < X < 1: \quad \frac{\partial^2 \theta_g}{\partial X^2} = \frac{R_{ep} P_r}{d_p/B} \frac{\partial \theta_g}{\partial x} - \Delta H^* \tag{A-1}$$

$$-\infty < X < 1: \quad \frac{\partial \theta_g}{\partial X} = -(M/R_{ep} P_r)(\theta_g - \theta_s) + \varepsilon_p (\alpha/uB) \Delta H^* \tag{A-2}$$

$$0 < X < \infty: \quad \frac{\partial^2 \theta_g}{\partial X^2} = \frac{R_{ep} P_r}{d_p/B} \frac{\partial \theta_g}{\partial X} - \Delta H^* \tag{A-3}$$

solid:

$$-1 < X < 0: \quad \frac{\partial^2 \theta_s}{\partial X^2} = -M(\lambda_g/\lambda_e)(B/d_p)(\theta_g - \theta_s) \tag{A-4}$$

Initial condition and boundary condition

$$X = -\infty: \theta_g = 1 \tag{A-5}$$

$$x = -1: \frac{\partial \theta_s}{\partial X} = -\frac{\varepsilon}{4N^*}(\theta_{s2}^4 - 1) - (\lambda_g/\lambda_e)\frac{\partial \theta_g}{\partial X} = 0 \tag{A-6}$$

$$x = 0: \frac{\partial \theta_s}{\partial X} + \frac{\varepsilon}{4N^*}(\theta_{s1}^4 - \theta_a^4) - (\lambda_g/\lambda_e)\frac{\partial \theta_g}{\partial X} = 0 \tag{A-7}$$

where

$$\theta = T/T_0, X = x/B, N_{up} = h_p d_p/\lambda_g \; R_{ep} = d_p \rho_g u/\mu$$

$$P_r = C_{pg}\mu/\lambda_g, M = N_{up} BS, N^* = \lambda_e/(4\sigma T_o^3 B)$$

$$\Delta H^* = (B^2/\lambda_g T_o) R \Delta H, \alpha = \lambda_g/C_{pg}\rho_g$$

The mass balance equations for species in Eqs. (10)-(12) are rewritten respectively as

$$-\infty < x < -1: \frac{\partial Y_j}{\partial x} + \frac{B}{\rho_g u} R_j M_j = 0 \tag{A-8}$$

$$-1 < x < 0: \frac{\partial Y_j}{\partial x} + \varepsilon_p \frac{B}{\rho_g u} R_j M_j = 0 \tag{A-9}$$

$$0 < x < \infty: \frac{\partial Y_j}{\partial x} + \frac{B}{\rho_g u} R_j M_j = 0 \tag{A-10}$$

Nomenclature

A_0, A_0'	=	constant in frequency factor	[cm^3/mol.*s]
B	=	thickness	[m]
C_{pg}	=	specific heat at constant pressure	[kJ/Kg*K]
E_0	=	activation energy	[J/mol.]
G_0	=	mass velocity	[Kg/s]
ΔH	=	heat of reaction	[kJ/mol.]
h_p	=	heat transfer coefficient	[kJ/m^2*s*K]
Q	=	heat flux	[kJ/m^2*s]
q	=	heat load	[W/m^2]
R	=	reaction rate	[mol./s]
S	=	specific surface area	[m^2/m^3]
S_u	=	laminar flame speed	[m/s]
T	=	temperature	[K]
u	=	superficial gas velocity	[m/s]
x	=	coordinate in flow direction	[m]
X	=	dimensionless coordinate in flow direction	[–]
Y	=	mass fraction of species	[Kg/Kg]
ε	=	emissivity	[–]
ε_p	=	porosity	[–]
θ	=	dimensionless temperature	[–]
λ_e	=	effective thermal conductivity	[kJ/m*s*K]
λ_g	=	conductivity of gas	[kJ/m*s*K]
μ	=	viscosity	[Kg/m*s]
ρ_g	=	density of gas	[Kg/m^3]
σ	=	Stefan-Boltzmann constant	[kJ/m^2*s*K^4]
Φ	=	equivalence ratio	[–]

<Subscripts>

a	=	atmosphere
0	=	initial
1	=	surface of porous ceramics (downstream side)
2	=	surface of porous ceramics (upstream side)
cond	=	conduction
g	=	gas
rad	=	radiation
s	=	solid

Literature cited

1) Andrews, G.E. and D. Bradly: *Combustion and Flame.* **19,** 275-288 (1972)

2) Golombok M., A. Prothero, L.C. Shirvill and L.M. Small: *Combustion Science and Technology* **70,** 203-223 (1991)
3) Itaya, Y., K. Miyoshi, S. Maeda and M. Hasatani: *Kagaku Kogaku Ronbunshu,* **16,** 56-63 (1990)
4) The Society of Chemical Engineers, Japan: Kagaku Kogaku Binran 4th ed., 71-74
5) The Society of Chemical Engineers, Japan: Kagaku Kogaku Binran 4th ed., 86-87
6) The Society of Chemical Engineers, Japan: Kagaku Kogaku Binran 5t ed., 355-356
7) The Society of Chemical Engineers, Japan: Kagaku Kogaku Binran 5th ed., 363
8) Melvin, G. and William, B.S.: *14th Symp on Comb,* 1109-1118 (1972)
9) Robert, C. Reid *et al.*: "The Properties of Gases and Liguids", 3rd ed., McGraw-Hill Gook Company
10) Roger A. Strahlow: "Combustion Fundamentals", McGraw-Hill Book Company
11) Smoot, L.D., W.C. Hecker and G.A. Williams: *Combustion and Flame,* **26,** 323-342 (1976)
12) Strachan, D., J. Dubois and G. Lestrat: *International Gas Research Conference Preprint,* 196-203 (1989)
13) Yagi, S., D. Kunii and N. Wakai: *AIChE j.,* **6,** 543-546 (1960)
14) Yoshinari, Y: J Patent H4-5859(1992)
15) Yoshizawa Y., K. Sasaki and R. Echigo: *Trans. JSME,* **52-482,** 3587-3593 (1986)